

Plural and multiple small-angle scattering from a screened Rutherford cross section

Alex F. Bielajew¹

Institute for National Measurement Standards, National Research Council of Canada, Ottawa K1A 0R6, Canada

Received 7 September 1993 and in revised form 7 January 1994

The object of this paper is to employ the screened Rutherford cross section to construct a charged-particle multiple-scattering theory that does not suffer from either the small step-size artefact associated with the conventional Molière multiple-scattering distribution or the large step-size instability of the theory of Keil et al. [Z. Naturforsch. 15a (1960) 1031]. An exact numerical solution to the Wentzel elastic-scattering integral is found for charged particle step-sizes less than about 3000 mean-free-paths. The new distribution contains explicitly the expected single and no-scattering distributions in the limit of small step-size, matches the standard Molière distribution for large step-sizes and is expressed in terms of simple functional forms and numerical tables that may be sampled quickly for use in Monte Carlo methods. The new distribution may be expressed entirely in terms of only two parameters – a “reduced” angle and the mean free path. The large-angle limit of the distribution is expressed analytically and compared to the results of Keil et al. and Molière. Despite the fact that the conventional Molière distribution is based upon the assumption that many interactions participate in the development of the multiple-scattering angle, it is found that Molière’s large-angle limit is mostly correct although the large-angle behaviour is dominated by one or two interactions! The design of a Monte Carlo electron transport algorithm that incorporates the unique features of the new distribution is discussed.

1. Introduction

Modern “high-energy” Monte Carlo electron-transport algorithms (e.g. EGS4 [1], ETRAN [2], ITS [3]) employ multiple-scattering theories and “condensed history” methods to model electron transport in order to avoid prohibitively long computation times. However, when multiple-scattering theories are employed in the vicinity of material interfaces, varying degrees of approximation are introduced [4]. In the case of EGS4, which employs the Molière multiple-scattering theory [5,6], electron transport step-lengths which violate Molière’s lower step-size limit are either not deflected or a numerical fitting procedure is applied to the Molière theory that is approximate and unsubstantiated. In the case of ETRAN, which employs the Goudsmit–Saunderson [7,8] formalism, small step-sizes are modeled by extrapolating the scattering angle for a small step from the scattering angle of a larger step. ITS takes much of its physics modelling from ETRAN including the ETRAN implementation of Goudsmit–Saunderson multiple scattering. However, for small steps near interfaces a Gaussian approximation to the multiple-scattering distributions is employed. It may be argued that the small step-size limit of a multiple-scattering theory should contain the no-scattering and single-scattering terms as dominant components, not Gaussian shapes that arise naturally from a large step-size analysis [6]. While the Goudsmit–Saunderson theory contains no explicit small step-size constraint, numerical convergence difficulties prevent its use in the small step-size regime. Although modifications ameliorating this problem have been discussed [9], they have not been incorporated into the general-purpose Monte Carlo codes.

¹ Corresponding author, tel. +1 613 993 2197, fax +1 613 952 9865, e-mail alex@irs.phy.nrc.ca.

The purpose of this work is to revisit Wentzel's analysis [10] and develop a numerical solution that is valid from zero to large step-size. The incentive to employ a Wentzel-type analysis is that the multiple-scattering distributions can be expressed in the form of a "reduced" angle related to the true multiple-scattering angle by a scale factor that contains both energy and material dependence. This is a useful feature that reduces the amount of calculation and table look-ups in repetitive calculations. The new distribution should match the standard Molière expansion at large step-size and be expressed in terms of simple functional forms that facilitate use in Monte Carlo calculations.

There have been previous attempts to provide expressions valid for the plural-scattering regime that match the lower step-size range of validity of Molière theory. Leisegang [11] introduced an approximate numerical procedure valid for small step-sizes but with an intrinsic numerical inaccuracy that increases with increased step-size. Keil et al. [12] were able to reduce Leisegang's numerical instabilities to the extent that their distributions and Molière's distribution are equally approximate (within about 3–4% in the forward direction) for 20 mean-free-paths.

Some recent work has addressed the issue of improving the Molière distribution using a Molière-type analysis. Although it is assumed that the Molière expressions are valid for multiple-scattering distributions starting at about 20 mean-free-paths, it has been found that discrepancies of the order of 6% occur in the peak of the distributions for step-sizes of this magnitude [13]. In that work, the corrected distributions were given in numerical form using the parameters, but not the approximations, of the Molière development. The Molière parameters relating real angles to reduced angles are either not defined for small path-lengths or are subject to numerical instabilities in that region. Therefore, a new approach is motivated that characterises the small path-length behaviour in a consistent way and matches smoothly with either Molière distributions or corrected distributions.

2. Small-angle scattering theory

Bothe [14] and Wentzel [10] have described a theory of small-angle multiple elastic scattering which provides the probability for scattering into an angle θ after a total path-length t :

$$f(\theta, t)\theta d\theta = d\theta \theta \int_0^\infty d\eta \eta J_0(\eta\theta) \exp\left(-\frac{2\pi N_A t}{A} \int_0^\infty d\chi \sigma(\chi) [1 - J_0(\eta\chi)]\right), \quad (1)$$

where J_0 is the Bessel function of zeroth order, N_A is Avogadro's number, A is the atomic weight, and t is given in g/cm^2 . Substituting the small-angle form of the Rutherford cross section, $\sigma(\chi) \propto (\chi^2 + \chi_\alpha^2)^{-2}$, where χ_α is a screening angle, results in:

$$f(\theta, \lambda)\theta d\theta = d\xi \xi \int_0^\infty dz z J_0(z\xi) e^{-\lambda[1-zK_1(z)]}, \quad (2)$$

where K_1 is the first-order modified Bessel function of the second kind, λ is the length of the particle step measured in mean free paths, $\lambda = 2\pi N_A t/A \int_0^\infty d\chi \sigma(\chi)$, and $\xi = \theta/\chi_\alpha$.

Eq. (2) has two important properties: normalisation to unity,

$$\int_0^\infty d\theta \theta f(\theta, t) = 1, \quad (3)$$

and the small step-size limit,

$$\lim_{\lambda \rightarrow 0} f(\theta, t)\theta d\theta = d\theta \theta e^{-\lambda} \left(\frac{\delta(\theta)}{\theta} + \frac{2\lambda}{(1 + \xi^2)^2} + O(\lambda^2) \right). \quad (4)$$

Another form that will be useful for later development can be obtained by extracting the unscattered forward amplitude. Thus Eq. (2) may be rewritten:

$$f(\xi, \lambda) \xi d\xi = d\xi \xi \left(e^{-\lambda} \frac{\delta(\xi)}{\xi} + (1 - e^{-\lambda}) \int_0^\infty dz z J_0(z\xi) j(\lambda, z) \right), \tag{5}$$

where $j(\lambda, z) = (e^{\lambda z K_1(z)} - 1) / (e^\lambda - 1)$. The above equation employs a definition of the Dirac delta-function, $\delta(\xi)/\xi = \int_0^\infty d\eta \eta J_0(\eta\xi)$, that is consistent with the Fourier-Bessel integral, $\int_0^\infty dt t J_0(t\xi) \int_0^\infty du u J_0(tu) F(u) = F(\xi)$. The sub-distribution, $d\xi \xi \int_0^\infty dz z J_0(z\xi) j(\lambda, z)$, represents a normalised probability conditional upon at least one scattering having taken place.

This report describes the solution of Eq. (5) treating λ and χ_α as arbitrary parameters. Some discussion of the choice of these parameters is presented later in this report.

2.1. Molière's large step-size approximation

The main purpose of this section is to demonstrate that Molière's expansion can be derived from Eq. (2). In the course of this demonstration, leading order correction terms for Molière's expansion will be presented. However, it will also be demonstrated that Molière's expansion is divergent without arbitrary cut-off parameters. The divergence is not eliminated through use of the correction terms, nor is it eliminated through use of Eq. (5) after application of Molière's approximations.

Molière considered this expansion valid for $\lambda > 23$. The function $1 - zK_1(z)$ is a monotonically increasing function of z on the range $0 \leq z < \infty$ with a value of zero at $z = 0$ and unity for $z \rightarrow \infty$. Therefore, in regions where λ is large, a good approximation to the integrand of Eq. (2) may be obtained by keeping the low order terms in an expansion of $1 - zK_1(z)$ about small values of z . The function $1 - zK_1(z)$ has the following asymptotic form for small z :

$$\lim_{z \rightarrow 0} [1 - zK_1(z)] = \left(\frac{z^2}{4}\right) \left[1 - 2\gamma - \ln\left(\frac{z^2}{4}\right)\right] + \frac{1}{2} \left(\frac{z^2}{4}\right)^2 \left[\frac{5}{2} - 2\gamma - \ln\left(\frac{z^2}{4}\right)\right] \dots \tag{6}$$

Keeping terms of this order, Eq. (2) becomes:

$$\begin{aligned} f(\varphi, B) \varphi d\varphi &= d\varphi \varphi \int_0^\infty d\mu \mu J_0(\varphi\mu) \\ &\times \exp \left\{ \left(-\frac{\mu^2}{4} + \frac{1}{B} \frac{\mu^2}{4} \ln \frac{\mu^2}{4} \right) + \frac{e^{1-2\gamma-B}}{2} \frac{\mu^2}{4} \left[-\frac{\mu^2}{4} + \frac{1}{B} \frac{\mu^2}{4} \left(\ln \frac{\mu^2}{4} - \frac{3}{2} \right) \right] \right\}, \end{aligned} \tag{7}$$

where the change of variables, $\xi = \varphi \sqrt{\lambda B}$, $s = \mu / \sqrt{\lambda B}$, $B - \ln B = 1 - 2\gamma + \ln \lambda$, where γ is Euler's constant (0.577 216...), has been effected. The term proportional to $e^{1-2\gamma-B}$ represents a correction to the Molière distribution.

Ignoring the correction term for the moment, one notes that the forward amplitude of $f(0, B)$ is unbounded. Once the integration variable exceeds $2 e^{B/2}$, the exponential increases and the integral diverges.

The presence of the correction term does not prevent the divergence nor does a reformulation using Eq. (5). The divergence is not caused by the unscattered forward amplitude but by the approximation in Eq. (6). The large- z asymptotic form of $1 - zK_1(z)$ is required to cure this anomaly.

Molière further approximated the distribution by making an expansion in B^{-1} :

$$f(\varphi, B) = 2 e^{-\varphi^2} + \sum_{n=1}^\infty \frac{f^{(n)}(\varphi)}{B^n}; \quad f^{(n)}(\varphi) = \frac{1}{n!} \int_0^\infty d\mu \mu J_0(\varphi\mu) e^{-\mu^2/4} \left(\frac{\mu^2}{4} \ln \frac{\mu^2}{4} \right)^n. \tag{8}$$

Again the divergent forward amplitude emerges as it can be shown that $f^{(n)}(0) \rightarrow \log^n n$ for large n . Although it is often considered that keeping only 3 terms in the Molière expansion is somewhat satisfactory for $\lambda > 23$, the presence of the divergences makes problematic the extension of Molière's

expression to smaller λ . Indeed, retaining higher order terms in B^{-1} worsens the divergences for small λ [13]! A three-term expansion at $\lambda \approx 23$ can be in error by up to 6%. The additional $O(z^2)$ correction term given above reduces the discrepancy to about 1% at $\lambda \approx 23$ although smaller λ 's still give difficulties somewhat reduced in magnitude.

In the previous work [13], numerical solutions for Eq. (2) were presented in terms of the Molière parameters B and φ . However, the parameter B cannot be employed for small path-lengths, and instabilities in the numerical solution in the vicinity of $B < 3$ were observed. The main motivation for this work is to present a solution that is valid for arbitrarily small path-lengths.

2.2. The large-angle limit

The large-angle asymptotic form of Eq. (5) can be determined directly. If one postulates that:

$$\lim_{\xi \rightarrow \infty} f(\xi, \lambda) = \frac{b(\lambda)}{\xi^4} + \frac{c(\lambda) \log \xi + d(\lambda)}{\xi^6} + O(\xi^{-8}), \quad (9)$$

where $b(\lambda)$, $c(\lambda)$ and $d(\lambda)$ are constants that depend only upon λ , then these constants can be determined by matching the factors of α in the following equation:

$$\lim_{\alpha \rightarrow 0} \{2b + \alpha[2d - \gamma c] - c\alpha \log \alpha\} = \lim_{\alpha \rightarrow 0} 4\alpha^2 \int_0^\infty d\xi \xi e^{-\alpha\xi^2} \int_0^\infty dz z J_0(z\xi) \left(e^{-\lambda[1-zK_1(z)]} \right). \quad (10)$$

The convergence factor $e^{-\alpha\xi^2}$ is employed to define the integral. The integral over ξ may be performed. Then a change of variables, $u = z^2/(4\alpha)$, gives:

$$\begin{aligned} \lim_{\alpha \rightarrow 0} \{2b + \alpha[2d - \gamma c] - c\alpha \log \alpha\} \\ = \lim_{\alpha \rightarrow 0} \int_0^\infty du e^{-u} (6 - 18u + 9u^2 - u^3) \frac{4}{\alpha} \left(e^{-\lambda[1-\sqrt{4\alpha u}K_1(\sqrt{4\alpha u})]} \right). \end{aligned} \quad (11)$$

Finally, an expansion of $\sqrt{4\alpha u}K_1(\sqrt{4\alpha u})$ in α may be performed using Eq. (6) allowing the identification of b , c and d with the result:

$$\lim_{\xi \rightarrow \infty} f(\xi, \lambda) = \frac{2\lambda}{\xi^4} \left(1 - \frac{2}{\xi^2} \right) - \frac{16\lambda^2}{\xi^6} (1 - \log \xi) + O(\xi^{-8}). \quad (12)$$

This is the identical limit obtained by Molière in his large path-length analysis except for the $-4\lambda\xi^{-6}$ term.

The above results suggest that the asymptotic behaviour may be obtained by an expansion of Eq. (5) in λ . This can be justified more fundamentally since it may be argued that the large-angle asymptotic behaviour develops through single or few scatterings as the probability for single large-angle scattering is very small. Thus, a wide-angle scattering comes predominantly from a single event rather than many small-angle events.

An expansion of Eq. (5) in terms of λ yields:

$$f(\xi, \lambda) = e^{-\lambda} \frac{\delta(\xi)}{\xi} + \frac{2\lambda}{(\xi^2 + 1)^2} + \frac{\lambda^2}{3} \left({}_2F_1\left(2, 3; \frac{5}{2}; \frac{-\xi^2}{4}\right) - \frac{6}{(\xi^2 + 1)^2} \right) + O(\lambda^3), \quad (13)$$

where ${}_2F_1()$ is the hypergeometric function^{#1}. The asymptotic behaviour of Eq. (13) is identical to that given in Eq. (12).

Apart from the small difference in the ξ^{-6} term there is a remarkable agreement between these results for the asymptotic behaviour and the asymptotic Molière results. Despite the large path-length

^{#1} The mathematical notation used in this report follows those of Wolfram [15], and the Mathematica code system was employed for most of the numerical computations reported herein.

development of the Molière expressions, the asymptotic forms which result from single and few scatterings are modeled accurately!

2.3. Small step-size approximation

Leisegang [11] introduced an approximation for the argument of the exponential in Eq. (2):

$$e^{zK_1(z)-1} = 0.368 + 0.742 e^{-0.914z} - 0.111 e^{-5.55z}. \quad (14)$$

and was able to solve Eq. (2) for integral values of λ introducing more approximations. Keil et al. have argued that Leisegang's results are useful for $\lambda \leq 4$ and introduced a refined approximation:

$$e^{zK_1(z)-1} = e^{-1} (1 + b_1 e^{-c_1 z} + b_2 e^{-c_2 z}), \quad (15)$$

with $b_1 = 2.10667$, $c_1 = 0.935$, $b_2 = -0.388388$, $c_2 = 5.000$. For integral values of λ , the use of approximation (15) reduces Eq. (2) to a double sum:

$$f(\theta, \lambda) \theta d\theta \approx d\xi \xi e^{-\lambda} \sum_{m=0}^{\lambda} \sum_{\mu=0}^{\lambda-m} \binom{\lambda}{m} \binom{\lambda-m}{\mu} \frac{b_1^m b_2^\mu (c_1 m + c_2 \mu)}{[(c_1 m + c_2 \mu)^2 + \xi^2]^{3/2}} \quad (16)$$

While Eq. (14) and Eq. (15) represent increasingly accurate numerical representations of the $\exp[zK_1(z) - 1]$ -factor in the integrand of Eq. (2) or Eq. (5), there are several difficulties with this approach. As λ increases, the error in the numerical approximation "compounds" because of the $\{\exp[zK_1(z) - 1]\}^\lambda$ -dependence. In the large-angle asymptotic region ($\xi \rightarrow \infty$) the behaviour of the approximate expressions become $e^\lambda \lambda (b_1 c_1 + b_2 c_2) \xi^{-3}$, not $O(\xi^{-4})$ as expected. The tail region ought to reproduce the single-scattering cross section tail for asymptotically large angles. This behaviour may be corrected by choosing $b_1 c_1 + b_2 c_2 = 0$ at the expense of reducing the quality of the fit to the function $e^{zK_1(z)-1}$. Alternatively, more parameters could be added to the fit. However, this approach was not pursued further herein. Finally, the $\lambda \rightarrow 0$ limit should produce the unscattered forward amplitude plus the single-scattering cross section evident in Eq. (4). The approximations do not, although the discrepancy in the forward direction is of the order of the numerical discrepancy in Eq. (14) and Eq. (15).

Further numerical approximations have been developed by Braicovich and Dupasquier [16] using the Leisegang numerical approach but employing a cross section that may be more suitable for the plural-scattering regime. Because of their numerical approximation their work is still subject to the difficulties described in the previous paragraph. Their use of a different (and more realistic) cross section is beyond the scope of this work which is dependent upon the functional form of the screened Rutherford cross section. However, with some effort their cross section may be implemented in the methodology introduced in the next section. This is left for future considerations.

3. An "exact" solution

Within the context of this paper, the "exact" solution is represented by the equivalent forms Eq. (2) or Eq. (5) recognising the fact that the screened Rutherford cross section is an approximation, the small-angle approximation to the screened Rutherford cross section is another approximation, and finally, the small-angle formalism of Wentzel's equation introduces another level of approximation. Bethe [17] and Winterbon [18] have discussed in detail corrections dealing with the last assumption. Corrections for the first two are beyond the scope of this work. It should be noted that the results of this work do not depend on the exact form of the screening angle or total cross section. Any form would suffice. The assumption of the small-angle Rutherford cross section, $d\sigma/d\theta \propto \theta/(\theta^2 + \chi_\alpha^2)^2$, is fundamental to the following development. Enhancements to this may take the form of a perturbation development, but this is not pursued herein.

Starting with the part of Eq. (5) that describes at least one scattering (the $1 - e^{-\lambda}$ term), consider the change of variables $u = 1 - \omega^2/(\xi^2 + \omega^2)$, where for the moment ω is arbitrary. Thus, the distribution that describes at least one scattering is:

$$q(u, \lambda, \omega) du = du \frac{\omega^2}{2(1-u)^2} \int_0^\infty dz z J_0(\omega z [u/(1-u)]^{1/2}) j(\lambda, z). \quad (17)$$

The distribution function $q(u, \lambda, \omega)$ has the properties $\int_0^1 q(u, \lambda, \omega) du = 1$, $q(0, \lambda, \omega) = \frac{1}{2}\omega^2 \int_0^\infty dz z j(\lambda, z)$ and $q(1, \lambda, \omega) = \lambda/[\omega^2(1 - e^{-\lambda})]$.

The motivation for the form of u is that $du = 2\omega^2 d\xi/(\xi^2 + \omega^2)^2$, which looks like a single-scattering angular distribution but with a "spreading" parameter, ω . Having chosen a form for ω as in the following development, the $q(u, \lambda, \omega)$ -distribution is the correction to this "spreading-single-scattering" approximation.

The parameter ω can be chosen to control the shape of $q(u, \lambda, \omega)$. Indeed, for efficacious numerical use, $q(u, \lambda, \omega)$ should be as "flat" as possible. Constructing the integrated square-amplitude:

$$r^2(\lambda, \omega) = \int_0^1 [q(u, \lambda, \omega) - 1]^2 du, \quad (18)$$

and minimising with respect to ω^2 yields the solution:

$$\omega_0^4(\lambda) = \frac{\int_0^\infty dz z [j''(\lambda, z) - j'(\lambda, z)/z]^2}{\int_0^\infty dz z j^2(\lambda, z)}, \quad (19)$$

where $j'(\lambda, z)$ and $j''(\lambda, z)$ are the first and second derivatives respectively of $j(\lambda, z)$ with respect to z . The parameter ω_0 is plotted in Fig. 1. In the limit of small path-lengths, $\omega_0(\lambda \rightarrow 0) \rightarrow 1$, and $q(u, 0, 1) = 1$ which describes the single-scattering limit. The minimised surface, $q_0(u, \lambda) = q(u, \lambda, \omega_0(\lambda))$ is plotted in Fig. 2 for $1/100 \leq \lambda \leq 3050.53$.

The shape of $q_0(u, \lambda)$ was reproduced with a single-scattering Monte Carlo code that was formulated in the small-angle approximation. Such a procedure can be recast in terms of the variable ξ and the distributions then depend only upon the number of mean free paths, λ . (Details are given in the Appendix.) A comparison is given in Fig. 3 for $\lambda = 0.1, 1, 10$ and 100 . 10^6 particle histories were simulated for each λ . For $\lambda < 1$ an "interaction-forcing" scheme [19] was employed to avoid wasted computer time on particles that do not scatter. To within statistics, the Monte Carlo calculations reproduce exactly the shape of $q_0(u, \lambda)$. Although the Monte Carlo results are expressed in terms of $u = 1 - \omega_0^2/(\xi^2 + \omega_0^2)$, the parameter ω_0 was not employed during the simulation. It was used simply to rescale the final scattering angle into the appropriate u -bin for comparison.

A comparison with the Molière 3-term distribution of Eq. (8) is given in Fig. 4 for $10 \leq \lambda \leq 3050.53$ and in Fig. 5 for selected values of λ . The maximum deviation ($|q_M(u, \lambda)/q_0(u, \lambda) - 1|$) of the Molière distribution is depicted in Fig. 6. The comparison with the Molière distribution demonstrates the appearance of spurious "wiggles" that are known to occur for small values of λ [13]. Andreo et al. [13] also demonstrated that errors of the order of 6% could be expected near the forward peak of the Molière distributions at $\lambda \approx 23$ and that result is corroborated here. If one demands that the Molière three-term distribution be "correct" to within 1%, then one must go to values of λ as high as 2000. The largest discrepancy generally occurs at $u \approx 0.88$, approaching the large-angle limit of the expressions. Recall that the Molière agreement at large angles was correct only to $O(\xi^{-4})$, there remaining a discrepancy of order $4\lambda/\xi^6$. It is likely that this and higher-order inaccuracies of the Molière expressions are causing this discrepancy.

A comparison with the Keil et al. distribution is given in Fig. 7 for $0.01 \leq \lambda \leq 100$ and in Fig. 8 for selected values of λ . The ratio of the Keil et al. distribution to the exact solution, $q_{KZZ}(u, \lambda)/q_0(u, \lambda)$, is given. The compounded error in the numerical approximation is evident as an increasing departure

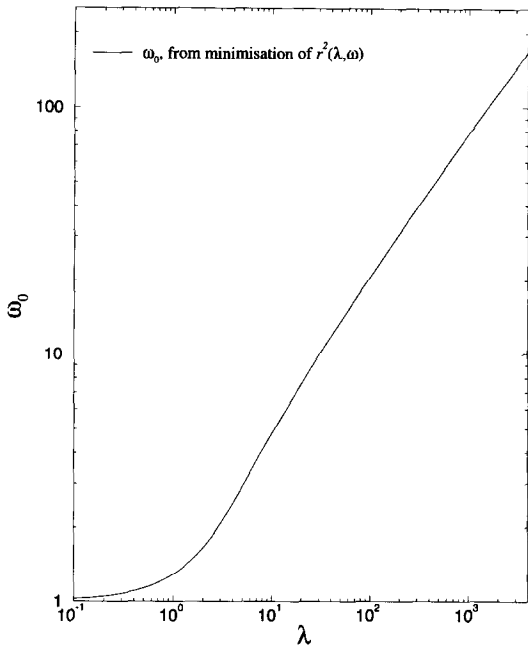


Fig. 1. The solution for $\omega_0(\lambda)$ based upon the minimisation of the integrated square-amplitude, $r^2(\lambda, \omega)$.

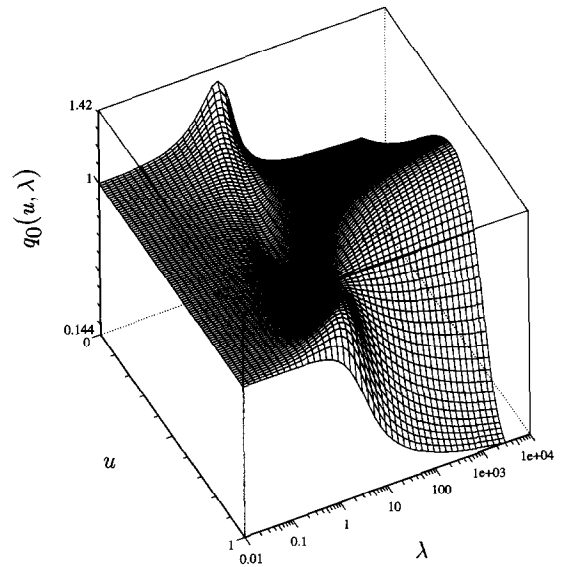


Fig. 2. The minimised $q_0(u, \lambda)$ vs. λ and u .

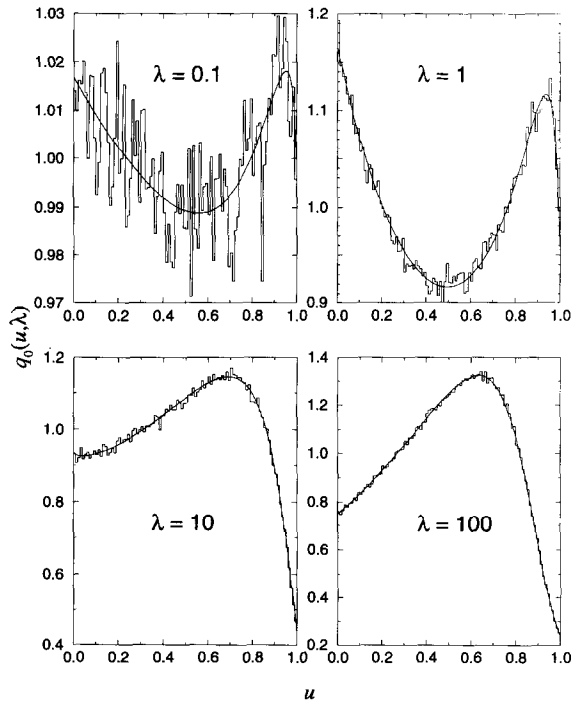


Fig. 3. The minimised $q_0(u, \lambda)$ vs. u for selected values of λ (curves) compared with small-angle Monte Carlo calculations (histograms).

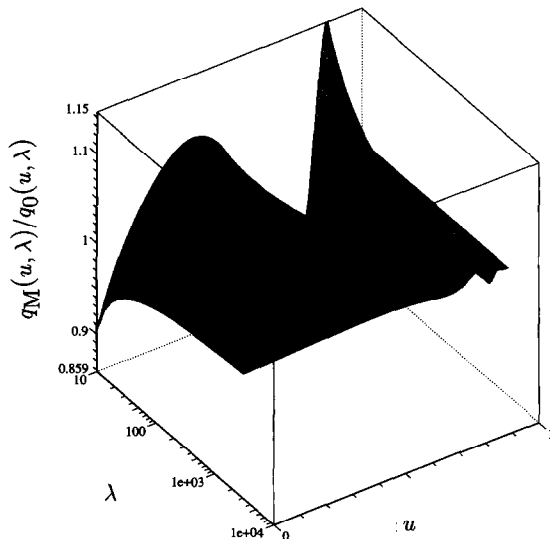


Fig. 4. The ratio of the Molière distribution, $q_M(u, \lambda)$, to the new distribution, $q_0(u, \lambda)$ vs. λ and u .

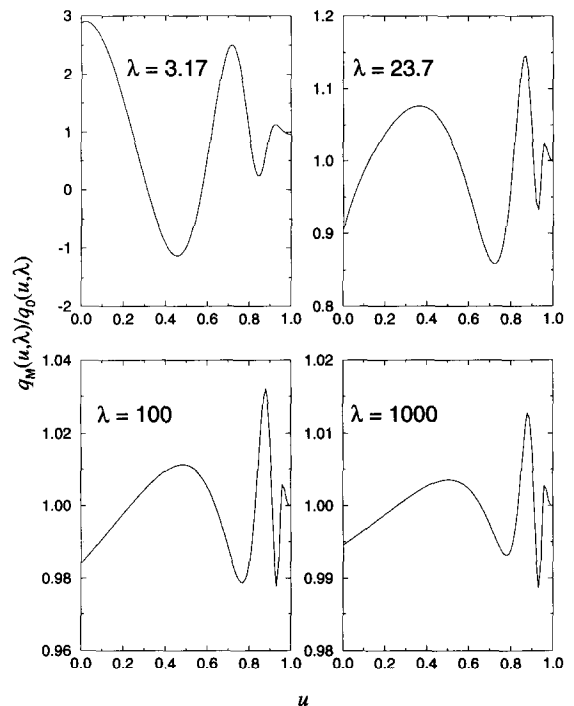


Fig. 5. The ratio of the Molière distribution, $q_M(u, \lambda)$, to the new distribution, $q_0(u, \lambda)$, for selected values of λ . The smallest value of λ corresponds to $e^{2\gamma}$, the minimum value for which the Molière expansion may be expressed. (Molière considered his theory valid above $\lambda \approx 23$, where he stated the accuracy to be about 1%.)

from unity with increased λ . The error in the large-angle asymptotic behaviour of the Keil et al. theory is evident at large angles. There is a broad plateau for small λ and small u . The region where the Keil et al. distribution is within 1% of the exact distributions is approximately $\lambda < 10$, $u < 0.7$. Owing to the difference in the asymptotic behaviours the ratio near $u \rightarrow 1$ becomes infinite. For this reason, the ratio only up to $u = 0.99$ is shown. In Fig. 7, only values of the ratio between 0.9 and 1.1 were depicted.

4. Application in a Monte Carlo transport algorithm

As discussed in the introduction, general-purpose Monte Carlo methods that employ multiple-scattering methods treat electron transport near interfaces in an approximate manner. Recent developments directed at this issue, EGS4/PRESTA [4] and ETRAN/TLC [20] still have difficulties with either the small step-size limit of Molière theory or numerical difficulties with the Goudsmit–Saunderson approach. With the new multiple-scattering method, a uniform and consistent approach may be taken. On the approach to an interface, the new method may be employed allowing particle steps to be reduced until the particle drifts to the interface boundary without scattering. Thus, no approximation is made at the interface surface. Once on the surface the particle can be transported using the mean-free path to a single elastic scattering, thereafter the new algorithm takes over.

This is illustrated in Fig. 9. A particle is directed at an interface between media A and B. The interface is a distance λ_f from the particle along its direction of motion and a perpendicular distance

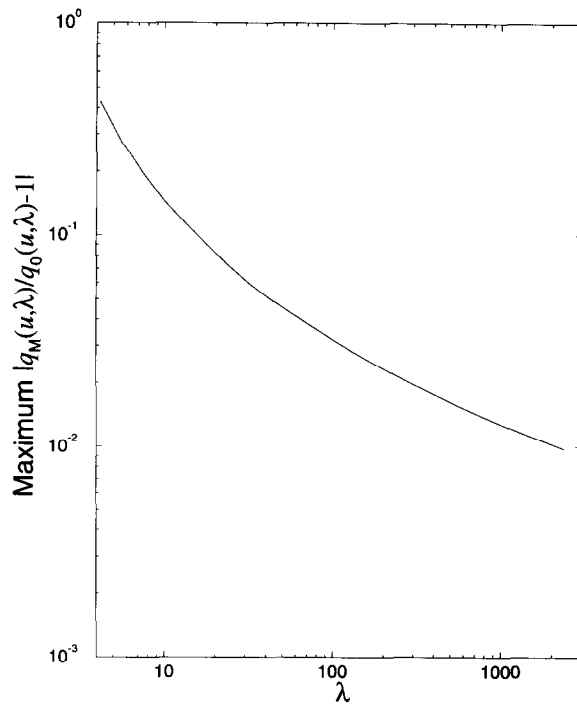


Fig. 6. The maximum deviation ($|q_M(u, \lambda)/q_0(u, \lambda) - 1|$) of the Molière distribution as a function of λ .

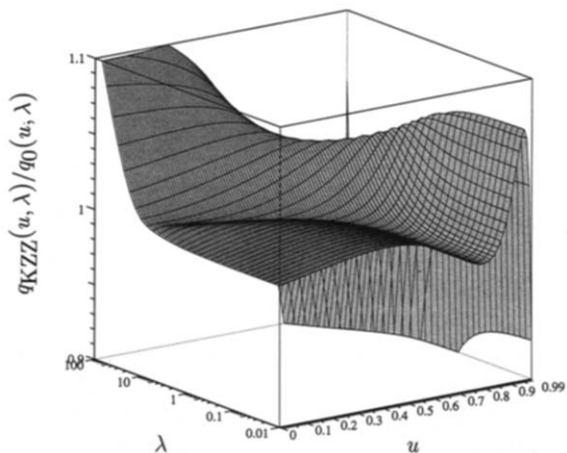


Fig. 7. The ratio of the Keil et al. distribution, $q_{KZZ}(u, \lambda)$, to the new distribution, $q_0(u, \lambda)$ vs. λ and u .

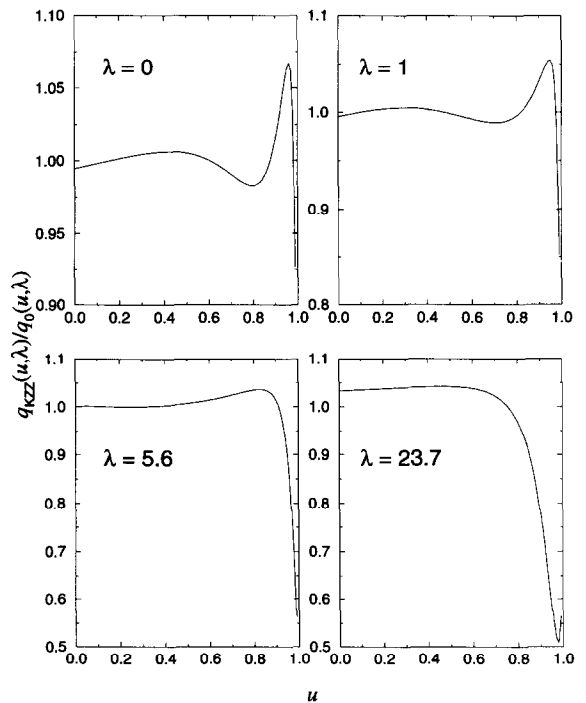


Fig. 8. The ratio of the Keil et al. distribution, $q_{KZZ}(u, \lambda)$, to the new distribution, $q_0(u, \lambda)$, for selected values of λ .

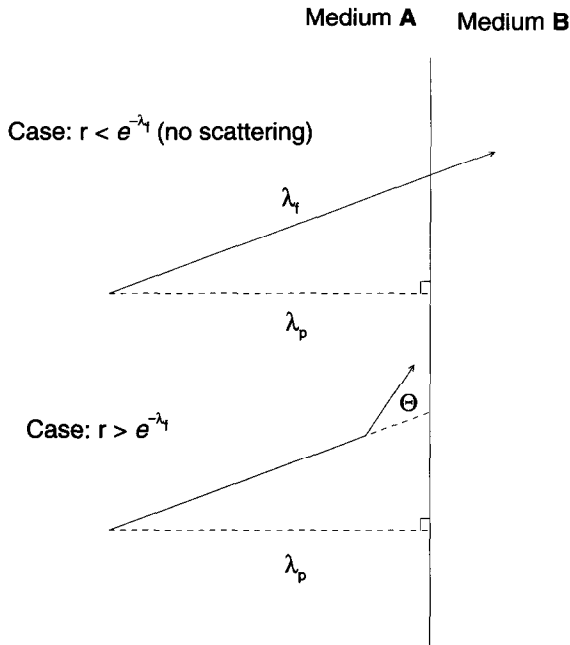


Fig. 9. Elements of a new Monte Carlo scheme that exploits the no-scattering drift feature of the small step-size limit of the new multiple-scattering scheme.

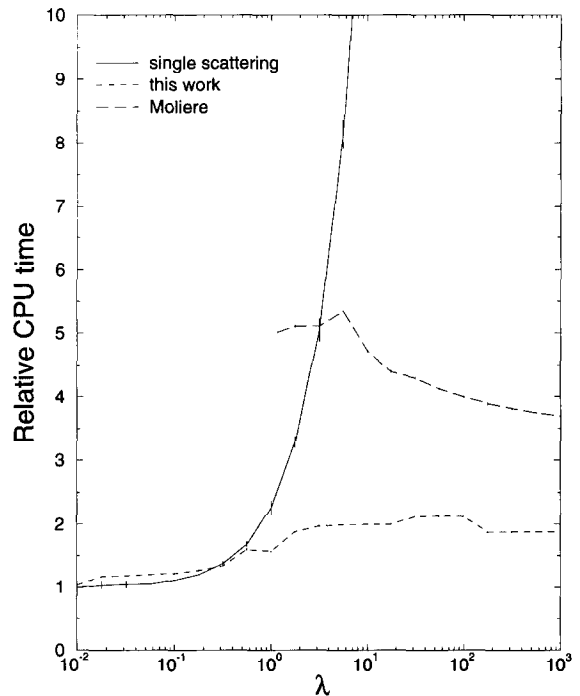


Fig. 10. Timing comparison between the single-scattering method, the new multiple-scattering method employing a fine mesh and the Molière method as extracted from the EGS4 code.

of λ_p from it. A random number r is chosen. If it is less than $e^{-\lambda_f}$, the particle is allowed to reach the interface surface without scattering. Otherwise, a step of length λ_p is taken and the particle is deflected by an angle calculated from the new method. Once on the interface the first step is chosen by sampling the single-scattering cross section. Thereafter, transport steps are chosen according to the algorithm described above.

While it seems wasteful if each particle step must calculate λ_p and λ_f for each particle step, only λ_p need to be calculated except in the very vicinity of the interface where an interface traversal seems imminent.

The new multiple-scattering distributions may be employed in several ways. However, for the purpose of routine sampling, the surface $q_0(u, \lambda)$ was calculated on a grid from $\lambda = 0.01$ to 3050.53 with 64 logarithmically-spaced divisions per decade. The grid in u was divided into 100 equally-spaced intervals. These data were then integrated to generate an inverse distribution $u(r, \lambda)$ where $r = \int_0^u du' q_0(u', \lambda)$ with the same grid spacing for λ and 100 equally-spaced intervals for r . (The numerical intergration was performed using an adaptive Romberg technique described by Press et al. [21].) During routine calculation, a random number r is selected and the $u(r, \lambda)$ data interpolated linearly to extract u . Then the scattering angle is related to u from the equation $\Theta = \chi_\alpha \omega_0(\lambda) \sqrt{u/(1-u)}$. The parameter $\omega_0(\lambda)$ is interpolated in a table with the same λ -density.

Despite the fact that a 150-kbyte table must be interpolated, timing studies on a variety of workstation-class computers showed that this technique samples about as quickly as the Molière method as extracted from the EGS4 code and in one case, a factor of 2 faster. (Results ranged from twice as fast to 5% slower.) A timing comparison for a Sun IPX computer is shown in Fig. 10. The general features should be similar on other computers. In a production-class code, the $u(r, \lambda)$ tables would be reduced to optimise interpolation to within a given accuracy thereby realising even more gains in execution speed. Compared to single-scattering sampling, the new method samples more

quickly starting at $\lambda \approx 1$ which indicates great potential for its use for all step-sizes. The timing degradation for even smaller step-sizes is probably not sufficient to warrant special coding for implementing a single scattering algorithm for the purpose of generating elastic-scattering angular distributions.

5. Discussion and conclusions

The Wentzel multiple-scattering theory has been recast into a form that does not suffer from the small step-size constraint associated with the conventional Molière expansion, that contains explicitly the expected single and no-scattering distributions in the limit of very small step-size and that does not rely on the numerical approximations of the Leisegang procedure that are problematic for large step-size and large angles. The new distribution matches the standard Molière expansion at large step-size and is expressed in terms of a simple functional form and numerical tables that may be sampled quickly for use in repetitive Monte Carlo methods. Sampling methods have been developed for Monte Carlo calculations that return scattering angles as quickly as the Molière method and is more efficient than a single-scattering method starting at a drift distance of the order of a single mean-free-path. The new distribution may be expressed entirely in terms of only two parameters – a “reduced” angle and the mean free path. Thus, the amount of numerical data is kept to a minimum, less than 150 kbytes for a fine mesh grid encompassing all energies and materials.

Although the Wentzel multiple-scattering method was used as a basis, the total cross section and screening angle were not employed directly. They are only employed to relate the reduced angle to real angles. These parameters may be taken from Molière’s theory, although Molière’s multiple-scattering theory has the same freedom of choice. More sophisticated approaches may be employed. For example, Fernández-Varea et al. [22] have considered these as free parameters that can be adjusted by the first and second transport cross sections obtained from partial-wave cross sections. Although it may be argued that the small-angle Rutherford functional form employed in this work is a significant approximation, the new distribution developed in the course of this work could be used as a basis for perturbative methods that model the single-scattering cross section more accurately. Other large-angle corrections, such as that discussed by Bethe and Winterbon may be incorporated directly. A more realistic cross section may be employed, such as that proposed by Braicovich and Dupasquier [16] and the six parameters of their theory may be employed directly or as fitting parameters to partial-wave cross sections. Their cross section is couched in a small-angle formalism and is amenable to the mathematical procedures developed in this paper.

The large-angle limit of the new distribution has been expressed analytically. Remarkably, the large-angle limit agrees closely with the results of Molière despite the fact that the conventional Molière distribution assumes that many interactions participate in the development of the multiple-scattering angle and that the large-angle behaviour is dominated by single large-angle interaction. However, the Leisegang numerical procedure causes a large discrepancy at large angles and this shortcoming has affected the large-angle behaviour of the Keil et al. theory and, presumably, that of Braicovich and Dupasquier who adopted similar approximations.

The design of a new electron transport algorithm that makes use of the correct small step-size no-scattering limit was discussed. Since the distribution is “universal” the step-sizes can be made so small as to enter the no-scattering limit and the particle may be allowed to drift to the boundary without approximation. In effect, although there is a shortcoming associated with the use of a small-angle screened Rutherford cross section, the consistency of the approach is maintained. There are two important applications where this consistency is critical.

Electron step-size artefacts have been discussed in detail in a previous report [4] and a general method for correcting artefacts associated with crossing boundaries was proposed. The solution required the shortening of electron transport steps in the vicinity of boundaries so that it would appear that most the transport steps occurred in an “infinite” medium. This procedure requires a multiple-scattering theory to be consistent since the transport step could be divided into segments of arbitrary

length. Even the optimum balance of Molière and Keil et al. theories has inconsistencies that may result in calculations differing depending on how the transport steps were subdivided. The consistent multiple-scattering theory developed herein does not suffer from this difficulty.

The other application is the calculation of ion chamber response to photon beams in the radiotherapy or diagnostic dosimetry [23,24]. Typically, an electron set in motion by a Compton or photoelectric event traverses the gas of an ion chamber in 2 or 3 elastic scatterings. However, for chambers with walls sufficiently thick, the electron fluence is in a state of quasi-equilibrium. As a consequence of near-equilibrium the fluence in the cavity is nearly independent of the difference in density between the ion chamber material wall and the cavity gas [25]. Thus, calculations of this phenomenon are sensitive to artificial sources of fluence perturbation that are produced by inconsistencies in the multiple-scattering theory as well as other aspects of the transport algorithm.

Although the new multiple-scattering theory, by virtue of its use of a simplistic single-scattering cross section, may have shortcomings when short step-size distributions are considered by themselves, its real advantage is to allow the arbitrary division of transport distances in a rigorously consistent manner.

6. Acknowledgements

The author would like to thank Dr. Pedro Andreo, University of Lund, Sweden, for discussions that motivated the completion of this work and for his assistance in using Mathematica, Dr. John Halbleib for his insight into the workings of ITS near interfaces, and Dr. Stephen Seltzer for the discussion on the inner working of ETRAN. Special thanks are given to Mr. Michael Muirhead for coding the small-angle Monte Carlo code used to verify the multiple-scattering distributions.

Appendix A. Small angle Monte Carlo calculations

The equations that relate the angles θ and ϕ with respect to some coordinate system before and after a scattering event can be expressed as:

$$\begin{aligned}\cos \theta' &= \cos \Theta \cos \theta - \sin \Theta \sin \theta \cos \Phi, \\ \sin \theta' \sin \phi' &= \cos \Theta \sin \theta \sin \phi + \sin \Theta (\cos \theta \cos \Phi \sin \phi + \sin \Phi \cos \phi), \\ \sin \theta' \cos \phi' &= \cos \Theta \sin \theta \cos \phi + \sin \Theta (\cos \theta \cos \Phi \cos \phi - \sin \Phi \sin \phi),\end{aligned}\tag{A.1}$$

where θ and ϕ are the laboratory polar and azimuthal angles before scattering, θ' and ϕ' are the laboratory angles after scattering, and the particle scatters by angles Θ and Φ . For general scattering, Φ can be measured relative to a particle transverse polarisation vector, but for elastic scattering the interaction is azimuthally symmetric and Φ is chosen uniformly over the range $[0, 2\pi]$.

In the small-angle approximation, all the polar angles are considered to be “small”. Thus the approximation is made: $\cos([\theta|\theta']|\Theta) \approx 1 - \frac{1}{2}[\theta|\theta']|\Theta]^2$ and $\sin([\theta|\theta']|\Theta) \approx [\theta|\theta']|\Theta$. This allows the scaling $\xi = \theta\chi_\alpha$, $\xi' = \theta'\chi_\alpha$ and $\Xi = \Theta\chi_\alpha$. The small-angle form of the deflection equation then becomes:

$$\begin{aligned}\xi' &= \sqrt{\xi^2 + \Xi^2 + 2\xi\Xi \cos \Phi}, \\ \xi' \sin \phi' &= \xi \sin \phi + \Xi \sin(\Phi + \phi), \\ \xi' \cos \phi' &= \xi \cos \phi + \Xi \cos(\Phi + \phi).\end{aligned}\tag{A.2}$$

This small-angle form of the deflection equations retains explicitly the normalisation of the azimuthal angle, $\sin^2 \phi' + \cos^2 \phi' = 1$ and depends only upon the scaled angle.

The iteration procedure then takes the form:

For the n^{th} -iteration:

- (i) Choose mean-free-path to next interaction from $e^{-\lambda}$, i.e. $\lambda_n = -\log r$ where r is a random number.
- (ii) If $\sum_{i=1}^n \lambda_i > \lambda$, exit iteration loop and accumulate final angle in a scoring array. Then, start over at $n = 1$. (λ is the total number of mean-free-paths for which the angular distribution is desired.)
- (iii) Choose Ξ from the normalised single-scattering cross section $d\sigma = 2\Xi d\Xi (\Xi^2 + 1)^{-2}$, i.e. $\Xi = \sqrt{r/(1-r)}$.
- (iv) Deflect particle according to Eq. (A.2).
- (v) Execute iteration $n + 1$.

This iteration procedure depends only upon λ and ξ and was employed to generate the Monte Carlo results depicted in Fig. 5.

References

- [1] W.R. Nelson, H. Hirayama and D.W.O. Rogers, The EGS4 Code System, Stanford Linear Accelerator Center Report SLAC-265 (Stanford, 1985).
- [2] S.M. Seltzer, An Overview of ETRAN Monte Carlo Methods, in: Monte Carlo Transport of Electrons and Photons Below 50 MeV, eds. W.R. Nelson, T.M. Jenkins, A. Rindi, A.E. Nahum and D.W.O. Rogers (Plenum, 1989) pp. 153–182.
- [3] J.A. Halbleib, R.P. Kensek, T.A. Mehlhorn, G.D. Valdez, S.M. Seltzer and M.J. Berger, ITS Version 3.0: The Integrated TIGER Series of Coupled Electron/Photon Monte Carlo Transport Codes, Sandia report SAND91-1634 (1992).
- [4] A.F. Bielajew and D.W.O. Rogers, Nucl. Instr. and Meth. B 18 (1987) 165.
- [5] G.Z. Molière, Z. Naturforsch 2 a (1947) 133.
- [6] G.Z. Molière, Z. Naturforsch 3 a (1948) 78.
- [7] S.A. Goudsmit and J.L. Saunderson, Phys. Rev. 57 (1940) 24.
- [8] S.A. Goudsmit and J.L. Saunderson, Phys. Rev. 58 (1940) 36.
- [9] M.J. Berger and R. Wang, Multiple-Scattering Angular Deflections and Energy-Loss Straggling, in: Monte Carlo Transport of Electrons and Photons Below 50 MeV, eds. T.M. Jenkins, W.R. Nelson, A. Rindi, A.E. Nahum and D.W.O. Rogers, (Plenum, 1989) pp. 21 – 56.
- [10] G. Wentzel, Ann. Phys. 69 (1922) 335.
- [11] S. Leisegang, Z. Phys. 132 (1952) 183.
- [12] E. Keil, E. Zeitler and W. Zinn, Z. Naturforsch 15 a (1960) 1031.
- [13] P. Andreo, J. Medin and A.F. Bielajew, Med. Phys. 20 (1993) 1315.
- [14] W. Bothe, Z. Phys. 5 (1921) 63.
- [15] S. Wolfram, Mathematica: a system for doing mathematics by computer (Addison-Wesley, Redwood City, 1991).
- [16] L. Briacovich and A. Dupasquier, Nuovo Cimento 56 (1968) 1066.
- [17] H.A. Bethe, Phys. Rev. 89 (1953) 1256.
- [18] K.B. Winterbon, Nucl. Instr. and Meth. B 21 (1987) 1.
- [19] A.F. Bielajew and D.W.O. Rogers, Variance-Reduction Techniques, in: Monte Carlo Transport of Electrons and Photons Below 50 MeV, eds. T.M. Jenkins, W.R. Nelson, A. Rindi, A.E. Nahum and D.W.O. Rogers (Plenum, 1989) p. 407.
- [20] S.M. Seltzer, Int. J. Appl. Radiat. Isotopes 42 (1991) 917.
- [21] W.H. Press, B.P. Flannery, S.A. Teukolsky and W.T. Vetterling, Numerical Recipes – The art of scientific computing (Cambridge University Press, Cambridge, 1986).
- [22] J.M. Fernández-Varea, R. Mayol, J. Baró and F. Salvat, Nucl. Instr. and Meth. B 73 (1993) 447.
- [23] A.F. Bielajew, D.W.O. Rogers and A.E. Nahum, Phys. Med. Biol. 30 (1985) 419.
- [24] D.W.O. Rogers, Med. Phys. 20 (1993) 319.
- [25] U. Fano, Radiat. Res. 1 (1954) 237.